Universiti Sains Malaysia RU Research Grant Technical Report

Title of Research Project:

The fabrication and investigation of diamond/zinc oxide heterojunction

Principle researcher:
Assoc Prof Dr Saw Kim Guan

Co-researchers:
1. Prof Zainuriah Hassan
2. Dr Yam Fong Kwong
3. Dr Ng Sha Shiong

Research Officer (Part-time):
Tneh Sau Siong

This work is funded by research grant RU 1001/PJJAUH/811057

Summary of outputs

A. Publications:
1) Ultraviolet photoresponse properties of zinc oxide on type IIb diamond heterojunction, *Physica B* (2010) 405 pp 4123- 4127.
2) Thermal degradation of single crystal zinc oxide and the growth of nanostructures, (2010) pp 43 – 46.
3) The structural and optical characterizations of ZnO synthesized using the "bottom-up" growth method, Physica B (2010) pp 2045 – 2048.
4) The effects of thermal treatments on microstructure phosphorus-doped ZnO layers grown by thermal evaporation, Composite Interfaces (2010) pp 863 – 872.

B. Conference Presentations: Zinc oxide/type IIb diamond heterojunction, Novel Aspects of surfaces and materials (NASM3), University of Manchester, 11 – 15 April 2010, Oral Presentation.

C. Training:
1) Research Officer – Tneh Sau Siong
2) PhD Students –
   (i) Tneh Sau Siong (Universiti Sains Malaysia)
   (ii) Javad Karamdel (collaboration with Universiti Kebangsaan Malaysia)

D. Networking and Linkages:
1. La Trobe University, Australia (as Honorary Academic Staff and for XPS and TOFSIMS measurements
2. Universiti Kebangsaan Malaysia (as fellow researcher)

E. Specific applications: A function p-n junction made from type IIb diamond and zinc oxide.

1. Introduction – why type IIb diamond is necessary

Zinc oxide (ZnO) and diamond are materials with wide energy band gaps of ~ 3.3 and 5.5 eV respectively and are thus attractive for opto-electronic applications. It is widely known that as-grown or undoped ZnO typically exhibits *n*-type conductivity. Although the source of free electrons contributing to the *n*-type conductivity has not been conclusively identified it is usually attributed to zinc interstitials, oxygen vacancies, hydrogen or even incorporated electronegative hydrogen carbonates [1-3]. Due to the compensation effect of a large *n*-type carrier concentration, *p*-type ZnO is extremely difficult to synthesize. Similarly, diamond rarely exhibits *n*-type conductivity and the doping process in diamond is difficult to achieve due to its compact lattice, allowing the diffusion of smaller or comparable species than carbon at reasonable temperature [4]. However, *p*-type conductivity is known to occur for type IIb diamond, in which boron is the dominant impurity in a concentration below 1 ppm. In principle, ZnO can thus be combined with type IIb diamond to make a *p-n* heterojunction. An added advantage is the mechanical and chemical stability as well as the high thermal conductivity of diamond (22 $Wcm^{-1}K^{-1}$), which is very useful in high temperature device applications. Despite this interesting possibility, ZnO on diamond heterojunction is difficult to synthesize as one of the crucial factors that could determine the successful fabrication of the ZnO on diamond heterojunction is the level of effective boron doping in diamond. Due to the small lattice constant of diamond, most doping elements would lead to severe distortions of the unit cell and are difficult to be incorporated. Only boron has been found to be suitable as an

acceptor donor, capable of forming a miniband, lowering the activation energy and enabling ohmic contacts by tunnelling. The activation energy of boron is $\Delta E_A = 0.37$ eV and boron activation at room temperature can be obtained although full activation is unlikely. It is believed that boron activation is possible either at low concentrations, when the Fermi level crosses the acceptor level or at high concentrations, when the miniband starts to overlap with the valence band [5]. At low boron concentrations, reasonable carrier activation can be obtained for doping level of 10^{13} cm^{-3} [5]. Interestingly, no rectifying behaviour is usually achieved for high levels of boron doping but current rectification has been observed for heterojunctions where diamond has been doped with residual boron [6]. Doping diamond with residual boron is a difficult task with uncertain results. Type IIb diamond, which is semiconducting by nature, has a low concentration of boron and could thus be used as a *p*-type material without the need for intentional doping with residual boron. Moreover, this material has been used in previous efforts to fabricate a bipolar transistor with some success [7].

2. Experimental details.

Type IIb natural diamond measuring 2.5 x 2.5 x 0.5 mm^3 was used in this work. The as-received diamond was cleaned using ethanol, acetone as well as deionized water sequentially in an ultrasonic bath and dried using pure nitrogen gas. No attempt was made to determine the concentration of the boron inclusion in the type IIb diamond but a concentration of below 1 ppm of boron or an estimated density of 10^{17} cm^{-3} has been known to cause *p*-type conductivity [8]. The surface of the diamond was partially sputtered with a thin film of ZnO ($\sim$ 500 nm) using a pure ZnO target in a pure argon atmosphere.

Current-voltage (I – V) measurements were performed in the dark and under UV illumination at room temperature using the Keithley I-V measurement system. The UV measurements were done under a 6 W UV lamp (λ = 372 nm) while the distance between the lamp and sample was 10 cm. X-ray photoelectron spectra were recorded using monochromatised Al Kα (1486.7 eV) x-ray radiation while micro-Raman spectroscopy and x-ray diffraction measurements were done using the Renishaw RN 1000 model and the PANalytical X'pert PRO high resolution x-ray diffractometer system respectively. An argon ion line at 514.5 nm was used as the excitation source for Raman measurements while the XRD measurements were performed with a fixed copper anode operating at 40 kV and 30 mA. The X-ray diffraction data was collected using Cu Kα radiation.

3. Results and Discussion

The low concentration of below 1 ppm of boron can be inferred from Raman measurements where the 1332.3 cm^{-1} diamond peak (FWHM = 4.5 cm^{-1}) was Lorentzian symmetric. The boron concentration was thus believed to be below the threshold of ~ 2 x 10^{20} cm^{-3}, the so-called Mott density, which corresponds to the onset of metallic conductivity [8-10]. A concentration above the threshold value will result in an asymmetric peak shape or the so-called Fano-like lineshape which is caused by a quantum mechanical interference between the zone-centre Raman active optical phonon and the continuum of electronic states induced by the dopant [10]. In addition the presence of boron was confirmed by the x-ray excited auger electron B KLL peak at the kinetic energy range of ~ 176 - 184 eV, which is within the range observed for the presence of boron [11].

The XRD pattern of the fabricated heterojunction shows the ZnO (002) and the diamond (111) peaks at $2\theta \sim 34.2^{o}$ and 44.6^{o} respectively. The former peak indicates the wurtzite ZnO hexagonal structure with lattice constants $a = 3.249$ Å and $c = 5.026$ Å. The SEM analysis indicates that the ZnO thin film is continuous. No contaminants were detected in the ZnO thin film by EDS analysis. In an earlier paper, we have reported the characterization of the sputtered ZnO thin films showing n-type conductivity [2].

I-V measurements of the In and Ni metal contacts are taken to ensure that ohmic contacts are established on the ZnO thin film and type IIb diamond respectively. The linear dependence of the I-V characteristics in indicates that ohmic contacts are fairly established after annealing the contacts in air in a controlled furnace at 600°C for 3 min.

From the I–V measurements, it is obvious that forward conduction occurs when the applied voltage reaches ~ 4.0 V for both dark and UV conditions. The diode turn-on can be interpreted as over a small range of voltages rather than occurring abruptly at the threshold voltage. The threshold voltages under dark and UV conditions are 5.9 and 5.5 V respectively. The UV illumination results in an increased current flow of an order higher. The relatively high voltages are probably due to the low ionization of the boron acceptors in diamond. The reverse breakdown voltages for the dark and UV light measurements are - 4.6 and – 6.6 V respectively. As the reverse bias reaches 10 V, the current for UV illumination is ~ 135 nA while only ~ 22 nA is observed for dark condition.

The change in the threshold voltage under UV illumination can be predicted using the following theoretical model. Since the ZnO on diamond heterojunction deviates from the case of an ideal I-V characteristic, the threshold voltage can be expressed as

$$V_{th} = V_D + IR_S \quad (1)$$

where V_D is the diffusion voltage and R_S is the series resistance for the device.

The diffusion voltage can be generally expressed as

$$eV_D = E_{g(diamond)} - (E_A + E_D) \quad (2)$$

where $E_{g(diamond)}$ is the energy bandgap of diamond while E_A and E_D are the boron acceptor level above the valence band in diamond and donor level in ZnO below the conduction band respectively. Taking the values of E_A and E_D as 0.37 and 0.38 eV respectively [12] we obtain $V_D = 4.72$ V for dark condition. Recalling that forward conduction occurs when the applied voltage reaches ~ 4.0 V and the extrapolated threshold voltage occurring at 5.9 V for dark condition, the diffusion voltage is within the expected value.

Under UV illumination, the electron-hole pairs are generated in ZnO thin film and the electrons subsequently affect the Fermi energy of *n*-ZnO. The change of the donor energy level ΔE_D in *n*-ZnO can be shown in Equation 4 below

$$\Delta E_D = \frac{kT}{q} \ln\left(\frac{N_{D_{dark}}}{N_{D_{dark}} + N_{D_{UV}}}\right) \quad (4)$$

where $N_{D_{dark}}$ = electron concentration of n-ZnO thin film under dark condition;
$N_{D_{UV}}$ = electron concentration of n-ZnO thin film under UV light.

The value of $N_{D_{dark}}$ obtained from Hall Effect measurements is 3.93 × 10^{16} cm^{-3} while $N_{D_{UV}}$ can be found from the photocurrent measurement as follows. Since the dimensions of the ZnO thin film are known, its volume under illumination can be easily obtained, which is ~ 1.17 × 10^{-7} cm^3. (Note that the ZnO material under the In contact is excluded). This gives the total volume of ZnO contributing to the photocurrent. The photocurrent that is caused by the UV illumination alone when the applied voltage is 0 V is

$$I = I_{UV} - I_{Dark} \quad (5)$$

By assuming that one photon creates only one electron-hole pair during UV illumination in ZnO and considering $e = 1.6\times10^{-19}\,\text{C}$, the number of electrons contributed by the volume of ZnO under UV illumination is estimated to be $n \sim 2.74\times10^{10}$. Thus the number of electrons caused by the breaking of the electron-hole pair under UV illumination per cm^3 is $n_{UV} \sim 2.33\times10^{17}\,\text{cm}^{-3}$. Subsequently we obtain $\Delta E_D \sim -50\ \text{meV}$. The negative sign implies that E_D has moved closer to the conduction band under UV illumination, resulting in an increased diffusion voltage. The diffusion voltage, V_D, under UV illumination is ~ 4.77 V. Assuming that the change in the mobility of charge carriers in ZnO is insignificant under UV illumination, we have

$$\left(\frac{N_{D_{dark}}}{N_{D_{dark}} + N_{D_{UV}}}\right) = \frac{R_{S_{(UV)}}}{R_{S_{(dark)}}} \quad (6)$$

Using the value of R_S = 5.6 x 10^7 Ω as obtained from the I-V measurement for dark condition we obtain the calculated value of $R_{S_{(UV)}}$, as 0.81 × 10^7 Ω. The calculated voltage threshold for dark condition $V_{th} = 5.51$ V can be obtained by using the corresponding

values of I = 14.1 nA and $V_D = 4.72$ V. Similarly, by using the values of I = 40.2 nA, $R_{S_{(UV)}} = 0.81 \times 10^7 \Omega$ and $V_D = 4.77$ V, the calculated voltage threshold under UV illumination is found to be 5.10 V. The difference in the voltage threshold values between dark condition and under UV illumination as calculated using this model is thus ~ 0.4 V, which is in agreement with the experimental results.

For the reverse bias, the saturation current of an ideal diode is due to the thermal generation of electron-hole pairs within a diffusion length on the either side of the transition region. The generated minority carriers subsequently move into the transition region and are swept to the other side of the junction by the electric field. Generation in the neutral regions would produce a typical saturation current that is essentially independent of reverse bias voltage. In materials with wide bandgaps, carrier generation can also occur within the transition (depletion) region itself. It is interesting to note that the reverse current of our ZnO on diamond heterojunction increases almost linearly with the square-root of bias voltage, suggesting that carrier generation is indeed taking place within the transition region. Under UV illumination, the increased generation of electron-hole pairs resulted in an increased reverse current.

References

[1] K. Vanheusden, W. L. Warren, C. H. Seager, D. R. Tallant, V. A. Voigt, B. E. Gnade, J. Appl. Phys. 79 (1996) 7983.

[2] K. G. Saw, K. Ibrahim, Y. T. Lim, and M. K. Chai, Thin Solid Films 515 (2007) 2879.

[3] C. G.. V. de Walle, Phys. Rev. Lett. 85 (2000) 1012.

[4] M. A. Pinault, J. Barjon, T. Kociniewski, F. Jomard, J. Chevallier, Physica B 401 – 402 (2007) 51.

[5] E. Kohn, A. Denisenko, Thin Solid Films 515 (2007) 4333.

[6] A. Hikavyy, P. Clauws, K. Vanbesien, P. De Visschere, O. A. Williams, M. Daenen, K. Haenen, J. E. Butler, T. Feygelson, Diamond and Relat. Mater. 16 (2007) 983.

[7] J. F. Prins, Appl. Phys. Lett. 41 (1982) 950.

[8] K. Thonke, Semicond. Sci. Technol. 18 (2003) S20.

[9] P. W. May, W. J. Ludlow, M. Hannaway, P. J. Heard, J. A. Smith, K. N. Rosser, Diamond and Relat. Mater. 17 (2008) 105.

[10] J. W. Ager, W. Walukiewicz , M. McCluskey, M. A. Plano, M. I. Landstrass, Appl. Phys. Lett. 66 (1995) 616.

[11] T. Mega, R. Morimoto , M. Morita, J. Shimomura, Surf. Interface Anal. 24 (1996) 375.

[12] C. X. Wang, G. W. Yang, C. X. Gao, H. W. Liu, Y. H. Han, J. F. Luo, G. T, Zou, Carbon 42 (2004) 317.

Physica B 405 (2010) 4123–4127

Contents lists available at ScienceDirect

Physica B

journal homepage: www.elsevier.com/locate/physb

Ultraviolet photoresponse properties of zinc oxide on type IIb diamond heterojunction

K.G. Saw*, S.S. Tneh, F.K. Yam, S.S. Ng, Z. Hassan

Nano-optoelectronics Research Laboratory, Universiti Sains Malaysia, Minden, 11800 Penang, Malaysia

ARTICLE INFO

Article history:
Received 20 May 2010
Accepted 29 June 2010

Keywords:
Zinc oxide
Diamond
Heterojunction
Ultraviolet photoresponse

ABSTRACT

Heterojunctions between ZnO and diamond are difficult to synthesize due to doping problems. In thi work, a successful heterojunction that is sensitive to ultraviolet (UV) light has been fabricated usin sputtered ZnO thin film on type IIb diamond, where boron activation at room temperature is possible a low concentrations. Current–voltage measurements show a p–n characteristic with significant U photoresponse properties. The threshold voltage under UV illumination is decreased by 0.4 V, whic can be predicted using a theoretical model.

© 2010 Elsevier B.V. All rights reserved

1. Introduction

Zinc oxide (ZnO) and diamond are materials with wide energy band gaps of ~3.3 and 5.5 eV, respectively, and are thus attractive for opto-electronic applications. It is widely known that as-grown or undoped ZnO typically exhibits n-type conductivity. Although the source of free electrons contributing to n-type conductivity has not been conclusively identified it is usually attributed to zinc interstitials, oxygen vacancies, hydrogen or even incorporated electronegative hydrogen carbonates [1–3]. Due to the compensation effect of a large n-type carrier concentration, p-type ZnO is extremely difficult to synthesize. Similarly, diamond rarely exhibits n-type conductivity and the doping process in diamond is difficult to achieve due to its compact lattice, allowing diffusion of species smaller than or comparable to carbon at reasonable temperature [4]. However, p-type conductivity is known to occur for type IIb diamond, in which boron is the dominant impurity at a concentration below 1 ppm. In principle, ZnO can thus be combined with type IIb diamond to make a p–n heterojunction. An added advantage is mechanical and chemical stability as well as the high thermal conductivity of diamond (22 W cm^{-1} K^{-1}), which is very useful in high temperature device applications. Despite this interesting possibility, ZnO on diamond heterojunction is difficult to synthesize as one of the crucial factors that could determine successful fabrication of the ZnO on diamond heterojunction is the level of effective boron doping in diamond. Due to the small lattice constant of diamond, most doping elements would lead to severe distortions of the unit cell and are difficult to be incorporated. Only boron has been found to b suitable as an acceptor or donor, capable of forming a minibanc lowering activation energy and enabling ohmic contacts b tunnelling. The activation energy of boron is ΔE_A=0.37 eV an boron activation at room temperature can be obtained althoug full activation is unlikely. It is believed that boron activation i possible either at low concentrations, when the Fermi leve crosses the acceptor level, or at high concentrations, when th miniband starts to overlap with the valence band [5]. At lov boron concentrations, reasonable carrier activation can b obtained for doping level of 10^{13} cm^{-3} [5]. Interestingly, n rectifying behavior is usually achieved for high levels of boro doping but current rectification has been observed for hetero junctions where diamond has been doped with residual boron [6 Doping diamond with residual boron is a difficult task wit uncertain results. Type IIb diamond, which is semiconducting b nature, has a low concentration of boron and could thus be use as a p-type material without the need for intentional doping wit residual boron. Moreover, this material has been used in previou efforts to fabricate a bipolar transistor with some success [7]. I this work, we report the fabrication of a heterojunction using as grown ZnO on type IIb diamond and its ultraviolet (UV photoresponse properties.

2. Experimental details

Type IIb natural diamond measuring 2.5 × 2.5 × 0.5 mm^3 wa used in this work. The as-received diamond was cleaned usin ethanol, acetone as well as deionized water sequentially in a ultrasonic bath and dried using pure nitrogen gas. No attempt wa made to determine the concentration of boron inclusion in th

* Corresponding author. Fax: +60 4 6576000.
E-mail addresses: kgsaw@usm.my, kgsaw@yahoo.com (K.G. Saw).

0921-4526/$ - see front matter © 2010 Elsevier B.V. All rights reserved.
doi:10.1016/j.physb.2010.06.064

ype IIb diamond but a concentration below 1 ppm of boron or an stimated density of 10^{17} cm^{-3} has been known to cause p-type onductivity [8]. The surface of the diamond was partially puttered with a thin film of ZnO (~500 nm) using a pure ZnO arget in a pure argon atmosphere.

Current–voltage (*I–V*) measurements were performed in the lark and under UV illumination at room temperature using a Keithley *I–V* measurement system. UV measurements were done under a 6 W UV lamp (λ=372 nm) while the distance between he lamp and the sample was 10 cm. X-ray photoelectron spectra were recorded using monochromatised Al Kα (1486.7 eV) X-ray adiation while micro-Raman spectroscopy and X-ray diffraction measurements were done using a Renishaw RN 1000 model and a PANalytical X'pert PRO high resolution X-ray diffractometer system, respectively. An argon ion line at 514.5 nm was used as the excitation source for Raman measurements, while the XRD measurements were performed with a fixed copper anode operating at 40 kV and 30 mA. The X-ray diffraction data were collected using Cu Kα radiation.

3. Results and discussion

Fig. 1(a) shows the Raman spectrum of the type IIb diamond. The low concentration of below 1 ppm of boron can be inferred from Raman measurements, where the 1332.3 cm^{-1} diamond peak (FWHM=4.5 cm^{-1}) was Lorentzian symmetric. Boron concentration was thus believed to be below the threshold of $\sim 2\times10^{20}$ cm^{-3}, the so-called Mott density, which corresponds to the onset of metallic conductivity [8–10]. A concentration above the threshold value will result in an asymmetric peak shape or the so-called Fano-like lineshape, which is caused by a quantum mechanical interference between the zone-centre Raman active optical phonon and the continuum of electronic states induced by the dopant [10]. Fig. 1(b) shows the X-ray excited Auger electron B KLL peak at the kinetic energy range ~176–184 eV, which is within the range observed for the presence of boron [11].

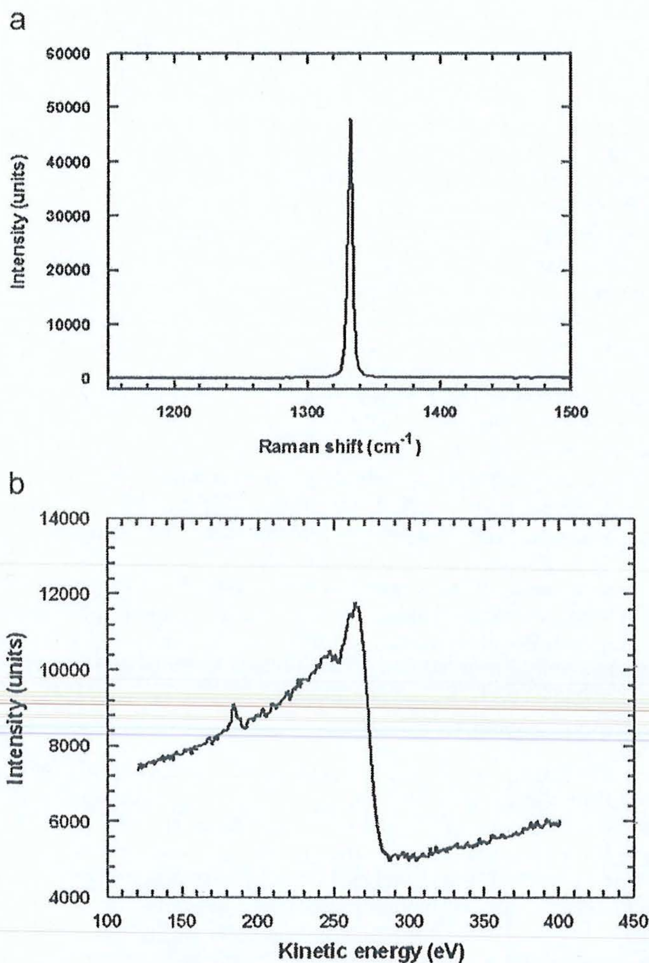

Fig. 1. (a) Raman spectrum of type IIb diamond and (b) the B KLL peak of the type IIb diamond, showing the presence of boron.

A schematic diagram of the ZnO on type IIb diamond heterojunction is shown in Fig. 2.

The XRD pattern of the heterojunction shows the ZnO (0 0 2) and the diamond (1 1 1) peaks at 2θ–34.2° and 44.6°, respectively (Fig. 3(a)). The former peak indicates the wurtzite ZnO hexagonal structure with lattice constants a=3.249 Å and c=5.026 Å. The SEM image in Fig. 3(b) shows the typical surface morphology of the continuous crystalline ZnO thin film prepared using d.c. sputtering. No contaminants were detected in the ZnO thin film by EDS analysis. Characterization of the sputtered ZnO thin films showing n-type conductivity had been reported previously [2].

I–V measurements of the In and Ni metal contacts are taken to ensure that ohmic contacts are established on the ZnO thin film and type IIb diamond, respectively. The linear dependence of the *I–V* characteristics in Fig. 4 indicates that ohmic contacts are fairly established after annealing the contacts in air in a controlled furnace at 600 °C for 3 min.

Fig. 5 shows the *I–V* measurements of the ZnO on type IIb diamond heterojunction performed in the dark as well as under UV light. The inset shows the spectrum of the UV lamp. From the *I–V* measurements, it is obvious that forward conduction occurs when the applied voltage reaches ~4.0 V for both dark and UV conditions. The diode turn-on can be interpreted as over a small range of voltages rather than occurring abruptly at the threshold voltage. Fig. 6(a) and (b) shows that the threshold voltages under dark and UV conditions are 5.9 and 5.5 V, respectively. The UV illumination results in an increased current flow of an order of magnitude higher. The relatively high voltages are probably due to low ionization of the boron acceptors in diamond. The reverse breakdown voltages for the dark and UV light measurements are −4.6 and −6.6 V (Fig. 6(c) and (d)), respectively. As the reverse bias reaches 10 V, the current for UV illumination is ~135 nA, while only ~22 nA is observed for dark condition.

The change in threshold voltage under UV illumination can be predicted as follows. Since the ZnO on diamond heterojunction deviates from the case of an ideal *I–V* characteristic, threshold

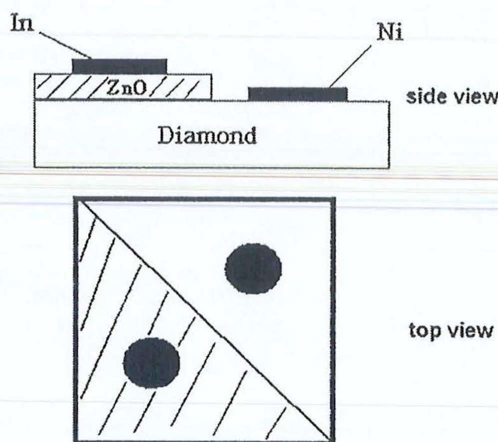

Fig. 2. Schematic diagram of ZnO on type IIb diamond heterojunction.

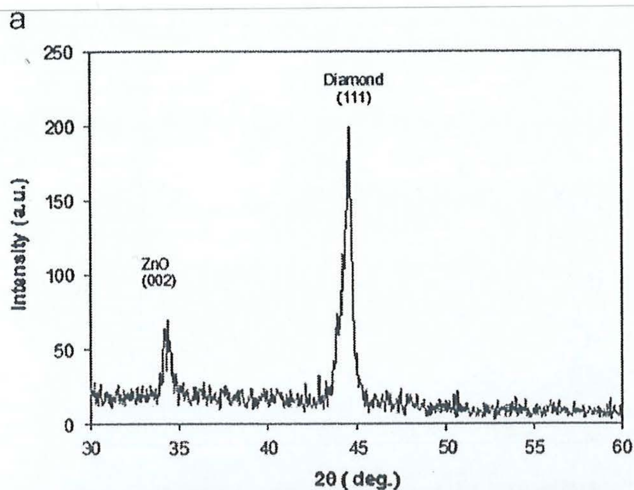

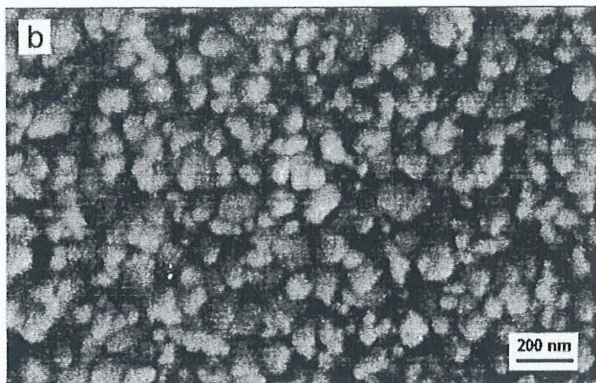

Fig. 3. (a) XRD pattern of ZnO on type IIb diamond heterojunction and (b) surface morphology of the ZnO thin film.

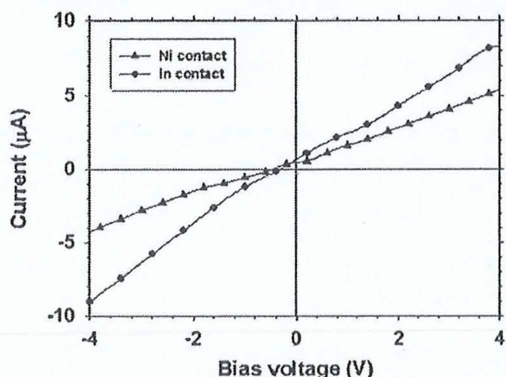

Fig. 4. *I–V* characteristics of In and Ni metal contacts on ZnO and type IIb diamond, respectively.

voltage can be expressed as

$$V_{th} = V_D + IR_S \quad (1)$$

where V_D is the diffusion voltage and R_S the series resistance for the device. The diffusion voltage shown in the energy band diagram (Fig. 7) can be generally expressed as

$$eV_D = E_{g(diamond)} - (E_A + E_D) \quad (2)$$

where $E_{g(diamond)}$ is energy bandgap of diamond while E_A and E_D are the boron acceptor level above the valence band in diamond and donor level in ZnO below the conduction band, respectively. Taking the values of E_A and E_D as 0.37 and 0.38 eV [12], respectively, we obtain V_D=4.72 V for dark condition. Recalling that forward conduction occurs when the applied voltage reaches ~4.0 V and the extrapolated threshold voltage occurring at 5.9 V for dark condition, the diffusion voltage is within the expected value.

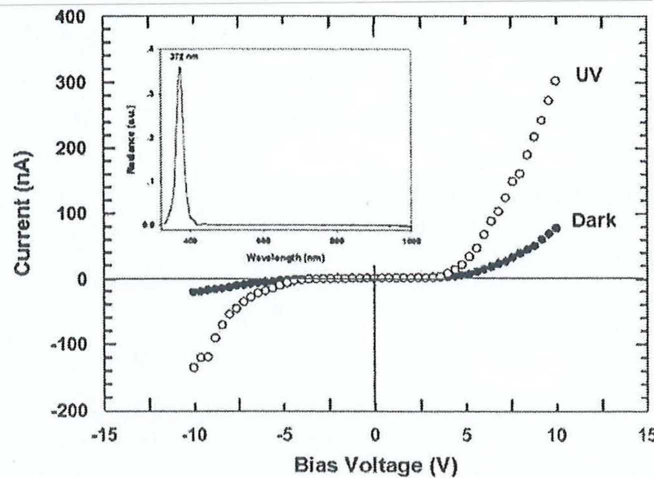

Fig. 5. *I–V* measurements showing a rectifying behavior of ZnO on type IIb diamond. UV illumination results in an increased current flow. Inset: UV spectrum of the UV lamp.

We assume that the diamond material is not significantly involved during the UV illumination because its bandgap is much larger than the energy of the UV light (3.33 eV) in this situation. With this assumption, Eq. (2) can be simplified to

$$e\Delta V_D = -\Delta(E_D) \quad (3)$$

Under UV illumination, electron–hole pairs are generated in the ZnO thin film and the electrons subsequently affect the Fermi energy of n-ZnO. The change of donor energy level ΔE_D in n-ZnO can be shown as follows:

$$\Delta E_D = \frac{kT}{q} \ln\left(\frac{N_{D_{dark}}}{N_{D_{dark}} + N_{D_{UV}}}\right) \quad (4)$$

where $N_{D_{dark}}$ is the electron concentration of *n*-ZnO thin film under dark condition and $N_{D_{UV}}$ the electron concentration of *n*-ZnO thin film under UV light.

The value of $N_{D_{dark}}$ obtained from Hall effect measurements is $3.93 \times 10^{16}\,cm^{-3}$ while $N_{D_{UV}}$ can be found from photocurrent measurement as follows. Since the dimensions of the ZnO thin film are known, its volume under illumination can be easily obtained, which is $\sim 1.17 \times 10^{-7}\,cm^3$. (Note that the ZnO material under the In contact is excluded.) This gives the total volume of ZnO contributing to the photocurrent. The photocurrent that is caused by the UV illumination alone when the applied voltage is 0 V is

$$I = I_{UV} - I_{dark} \quad (5)$$

By assuming that one photon creates only one electron–hole pair during UV illumination in ZnO and considering $e = 1.6 \times 10^{-19}$ C, the number of electrons contributed by the volume of ZnO under UV illumination is estimated to be $n \sim 2.74 \times 10^{10}$. Thus the number of electrons caused by the breaking of the electron–hole pair under UV illumination per cm^3 is $n_{UV} \sim 2.33 \times 10^{17}\,cm^{-3}$. Subsequently we obtain $\Delta E_D \sim -50$ meV. The negative sign implies that E_D has moved closer to the conduction band under UV illumination, resulting in an increased diffusion voltage. The diffusion voltage, V_D, under UV illumination is ~4.77 V. Assuming that the change in the mobility of charge

Fig. 6. (a) Threshold voltage for dark condition, (b) threshold voltage for UV illumination, (c) reverse breakdown voltage for dark condition and (d) reverse breakdown voltage for UV illumination.

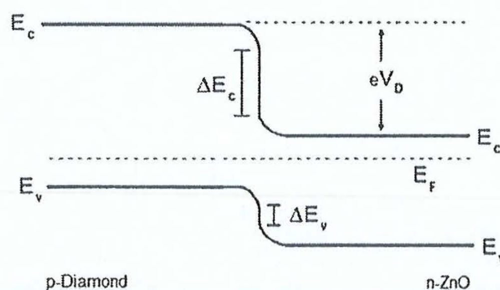

Fig.7. Energy band diagram of ZnO on type IIb diamond heterojunction.

carriers in ZnO is insignificant under UV illumination, we have

$$\left(\frac{N_{D_{dark}}}{N_{D_{dark}}+N_{D_{UV}}}\right)=\frac{R_{S_{(UV)}}}{R_{S_{(dark)}}} \tag{6}$$

Using the value $R_S=5.6\times10^7\,\Omega$ as obtained from the I–V measurement for dark condition we obtain the calculated value of $R_{S(UV)}$, as $0.81\times10^7\,\Omega$. The calculated voltage threshold for dark condition $V_{th}=5.51$ V can be obtained by using the corresponding values of $I=14.1$ nA and $V_D=4.72$ V. Similarly, using the values $I=40.2$ nA, $R_{S(UV)}=0.81\times10^7\,\Omega$ and $V_D=4.77$ V, the calculated voltage threshold under UV illumination is found to be 5.10 V. The difference in voltage threshold values between dark condition and under UV illumination as calculated using this model is thus ~0.4 V, which is in agreement with the experimental results.

In the reverse bias, the saturation current of an ideal diode is due to thermal generation of electron–hole pairs within a diffusion length on either sides of the transition region. The generated minority carriers subsequently move into the transition region and are swept to the other side of the junction by the electric field. Generation in the neutral regions would produce a typical saturation current that is essentially independent of reverse bias voltage. In materials with wide bandgaps, carrier generation can also occur within the transition (depletion) region itself. It is interesting to note that the reverse current of our ZnO on diamond heterojunction increases almost linearly with the square-root of bias voltage, suggesting that carrier generation is indeed taking place within the transition region. Under UV illumination, the increased generation of electron–hole pairs resulted in an increased reverse current.

4. Conclusion

In summary, we have successfully fabricated a ZnO on type IIb diamond heterojunction where a rectifying behavior is observed. A good response to UV illumination is evident from the I–V

characteristics in both the forward and reverse bias conditions, probably due to the photogeneration of additional electron–hole pairs.

Acknowledgements

This work was supported by an RU Research Grant (1001/PJJAUH/811057). The authors would like to thank Dr. P. Spizzirri from the University of Melbourne for the Raman measurements.

References

[1] K. Vanheusden, W.L. Warren, C.H. Seager, D.R. Tallant, V.A. Voigt, B.E. Gnade, J. Appl. Phys. 79 (1996) 7983.
[2] K.G. Saw, K. Ibrahim, Y.T. Lim, M.K. Chai, Thin Solid Films 515 (2007) 2879.
[3] C.G.V. de Walle, Phys. Rev. Lett. 85 (2000) 1012.
[4] M.A. Pinault, J. Barjon, T. Kociniewski, F. Jomard, J. Chevallier, Physica B 401 (2007) 51.
[5] E. Kohn, A. Denisenko, Thin Solid Films 515 (2007) 4333.
[6] A. Hikavyy, P. Clauws, K. Vanbesien, P. De Visschere, O.A. Williams, M. Daenen, K. Haenen, J.E. Butler, T. Feygelson, Diamond Relat. Mater. 16 (2007) 983.
[7] J.F. Prins, Appl. Phys. Lett. 41 (1982) 950.
[8] K. Thonke, Semicond. Sci. Technol. 18 (2003) S20.
[9] P.W. May, W.J. Ludlow, M. Hannaway, P.J. Heard, J.A. Smith, K.N. Rosser, Diamond Relat. Mater. 17 (2008) 105.
[10] J.W. Ager, W. Walukiewicz, M. McCluskey, M.A. Plano, M.I. Landstrass, Appl. Phys. Lett. 66 (1995) 616.
[11] T. Mega, R. Morimoto, M. Morita, J. Shimomura, Surf. Interface Anal. 24 (1996) 375.
[12] C.X. Wang, G.W. Yang, C.X. Gao, H.W. Liu, Y.H. Han, J.F. Luo, G.T. Zou, Carbon 42 (2004) 317.

Thermal Degradation of Single Crystal Zinc Oxide and the Growth of Nanostructures

K.G. Saw, [1,*] G.L. Tan, [1] Z. Hassan, [2] F.K. Yam, [2] S.S. Ng [2]

[1] *Physics Section, School of Distance Education, Universiti Sains Malaysia, 11800 Penang, Malaysia*
[2] *Schools of Physics, Universiti Sains Malaysia, 11800 Penang, Malaysia*
[*] *Corresponding author, Tel: +604 6534564; Fax: +604 6576000; e-mail: kgsaw@usm.my.*

Abstract. Heat treatment of (0001) single crystal zinc oxide (ZnO) seems to degrade the surface morphology at high temperature. The degradation, however, does not suppress the growth of ZnO nanostructures on selective regions of the single crystal ZnO that have been sputtered with metallic zinc (Zn) and annealed at 800°C. On the uncoated regions, no growth occurs but the presence of pits suggests material loss from the surface. The formation of ZnO nanostructures on the selective regions could be aided by the preferential loss of oxygen as well as zinc suboxides from the uncoated regions. Indirect evidence of the role of oxygen and zinc suboxides can be inferred from the formation of nickel zinc oxide $Ni_{0.9}Zn_{0.1}O$ and nickel oxide NiO_2 when Zn is replaced by Ni and annealed under similar conditions.

Keywords: zinc oxide, thermal degradation, nanostructures.

INTRODUCTION

The recent availability of large area single crystal ZnO has attracted much interest due to its potential applications in optoelectronics devices. It has a wide direct band gap of ~ 3.4 eV, a high exciton binding energy of ~ 60 meV at room temperature as well as the possibility of forming various types of nanostructures. The (0001) single crystal ZnO has a hexagonal wurtzite structure which consists of alternating planes of fourfold-coordinated Zn^{2+} and O^{2-} ions stacked along the *c*-axis. If the ZnO crystal is cut perpendicular to the *c* axis a Zn-terminated or (0001) surface is created on one side of the crystal and an O-terminated or $(000\bar{1})$ surface on the other. Studies on the effect of heat treatment on the (0001) single crystal ZnO are inconclusive despite the necessity to understand the accompanying changes on the surface morphology and other properties for the realization of ZnO based device technologies [1 – 4]. Although ZnO has a high melting point of 1975°C thermal degradation of surface morphology and electrical properties of single crystal ZnO at lower temperatures has been reported previously [2]. In this article, we report the effect of heat treatment on (0001) single crystal ZnO and the growth of ZnO nanostructures on specific regions of the ZnO wafer itself. While thermal degradation can have a detrimental effect on some potential applications, it can be surprisingly supportive of site specific growth of nanostructures.

CP1250, *Progress of Physics Research in Malaysia - PERFIK2009*, edited by A. K. Yahya
© 2010 American Institute of Physics 978-0-7354-0797-8/10/$30.00

Downloaded 09 Aug 2010 to 120.140.165.87. Redistribution subject to AIP license or copyright; see http://proceedings.aip.org/proceedings/cpcr.jsp

EXPERIMENTAL DETAILS

Mirror-polished single crystal (0001) ZnO wafers measuring 10 × 10 × 0.5 mm were used. The as-received wafers were cleaned ultrasonically using solvents before being annealed at 600 and 800°C in nitrogen or oxygen gas for 2 h at a flow rate of 4 L min^{-1} to study the extent of thermal degradation. To investigate the possibility of site specific growth of ZnO nanostructures, a thin film of Zn (~1 um) was sputtered onto selective regions of the (0001) wafer in argon with the aid of a mask. The sample was then inserted into a furnace and annealed at 800°C in an atmosphere of flowing nitrogen gas for 2 h. The possible role of oxygen loss and Zn_xO ($x>1$) from the ZnO wafer surface was investigated by depositing a Ni thin film on the selective regions instead of Zn and annealing it under similar conditions.

RESULTS AND DISCUSSION

The (0001) surface annealed at 600°C in nitrogen shows an approximate two-fold increase in the rms roughness of the surface. The increase in the surface roughness indicates degradation of the surface morphology. Similar results are observed for the $(000\bar{1})$ surface annealed under the same conditions. Many pits could be detected by SEM on the (0001) surface when it is annealed at 800°C in oxygen as well as nitrogen gas. Fig. 1 shows the thermally degraded (0001) surface. A rapid uneven loss of material from the surface is probably the cause of these pits. However, the SEM analysis could not detect any pits on the $(000\bar{1})$ surface that has been annealed. The rms roughness of the (0001) and $(000\bar{1})$ surfaces is 29.14 and 34.38 nm, respectively. Compared to the as-received wafer both annealed surfaces showed a significant increase in surface roughness of ~17 times.

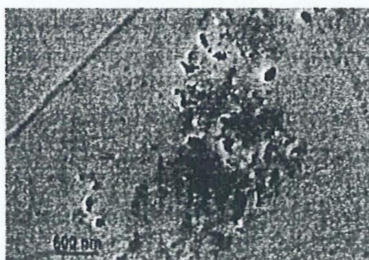

FIGURE 1. SEM image of the (0001) surface annealed at 800°C in a nitrogen ambient.

Annealing the (0001) single crystal ZnO that has been pre-coated with Zn thin film on selective regions results in the growth of ZnO nanostructures. The flake-like Zn grains are transformed into ZnO nanostructures after annealing in nitrogen at 800°C for 2h. Fig. 2 shows a nanomesh structure while the inset is SEM image showing a typical uncoated surface region on the single crystal ZnO wafer (A) and a typical region pre-coated with Zn (B).

Downloaded 09 Aug 2010 to 120.140.165.57. Redistribution subject to AIP license or copyright; see http://proceedings.aip.org/proceedings/cpcr.jsp

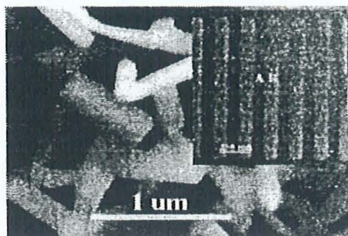

FIGURE 2. A nanomesh structure growing on the (0001) single crystal ZnO surface. Inset shows the selective regions of pre-coated Zn thin film on the single crystal ZnO.

Strong ultraviolet (UV) emission at ~ 377 nm and a weak broad emission at ~ 540 nm in the room temperature PL spectrum indicate that the ZnO nanostructures have a high crystalline structure. The position and intensity of the UV peak is similar to that obtained from the as-received single crystalline ZnO wafer. The broad emission band is not detected in the as-received single crystal ZnO spectrum. Fig. 3 shows the PL spectrum of the ZnO nanostructures while the inset shows the comparison of the as-received wafer and the uncoated region of the ZnO wafer after annealing. The uncoated regions of the annealed ZnO wafer show a much reduced near band edge emission and a distinct broad defect related peak. Defects caused by the desorption of oxygen and the diffusion of Zn atoms during the annealing process may act as non-radiative recombination centres and suppress the near band edge emission. The oxidation of the flake-like Zn grains into ZnO is confirmed by XRD analysis, which does not reveal any Zn peaks but the typical (002) and (004) ZnO peaks. In addition, the (022) and (440) peaks of zinc hydroxide carbonate $Zn_5(CO_3)_2(OH)_6$ are also present, suggesting that some hydrocarbons from the residual air in the furnace has been incorporated into ZnO during the annealing process. This is not surprising as ZnO has a high affinity for hydrocarbons.

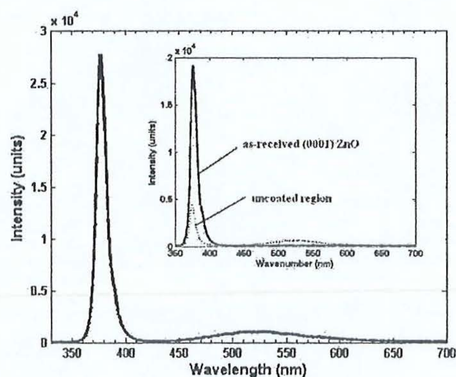

FIGURE 3. PL spectrum of the ZnO nanostructures while the inset shows the comparison of the as-received wafer and the uncoated region of the ZnO wafer after annealing.

Downloaded 09 Aug 2010 to 130.140.165.87. Redistribution subject to AIP license or copyright; see http://proceedings.aip.org/proceedings/cpcr.jsp

No growth occurs on the uncoated surface regions of the ZnO wafer. Instead irregular pits are seen, suggesting that Zn_xO and O could have evaporated from these regions [5] and diffuse into the nearby Zn-coated regions. Although the melting point of pure Zn metal is ~ 419°C, native oxides in the Zn thin film could have suppressed the rapid evaporation of Zn. This gives the metallic Zn time to react with the diffused oxygen to form ZnO nanostructures. Indirect evidence of the evaporation of oxygen and Zn_xO can be inferred from XRD analysis when the Zn thin film in the selective regions is replaced by Ni and annealed under similar conditions. The XRD pattern (not shown here due to lack of space) reveals the intense peaks due to the underlying ZnO wafer as well as $Ni_{0.9}Zn_{0.1}O$ whose (111), (200) and (220) peaks are found at $2\theta \sim 37.2^o$, 43.2^o and 62.7^o, respectively. The formation of $Ni_{0.9}Zn_{0.1}O$ suggests that oxygen and Zn_xO from the uncoated regions of the ZnO wafer have reacted with Ni. Two smaller peaks are also detected at $2\theta \sim 44.3^o$ and $\sim 64.5^o$ and are attributed to the presence of (111) Ni and (018) nickel oxide (NiO_2) respectively. The presence of (111) Ni implies that some Ni remains in the metallic state. In addition, some NiO_2 is also formed as a result of the reaction of Ni and oxygen from the uncoated regions of the ZnO wafer during the annealing process.

CONCLUSIONS

Heat treatment of single crystal ZnO results in its degradation. However, the degradation does not seem to suppress the growth of ZnO nanostructures on selective regions pre-coated with Zn and annealed at high temperature. The ZnO nanostructures possess a high crystalline structure with a (002) preferential growth direction and a strong ultraviolet emission at room temperature. The formation of nickel zinc oxide $Ni_{0.9}Zn_{0.1}O$ when a thin film of Ni is deposited on the selective regions instead of Zn suggests that evaporated oxygen and Zn_xO from the single crystal ZnO wafer could have supported the formation of ZnO nanostructures.

REFERENCES

1. V. A. Coleman, H. H. Tan. C. Jagadish, S. O. Kucheyev, and J. Zau, *Appl. Phys. Lett.* **87**, 231912 (2005).
2. R. Khanna, K. Ip, Y. W. Heo, D. P. Norton and S. J. Pearton, *Appl. Phys. Lett.* **85**, 3468-3470 (2004).
3. Z. Q. Chen, S. Yamamoto, M. Maekawa, A. Kawasuso, X. L. Yuan and T. Sekiguchi, *J. Appl. Phys.* **94**, 4807-4812 (2003).
4. T. Sekiguchi, S. Miyashita, K. Obara, T. Shishido and N. Sakagami, *J. Cryst. Growth* **214** 72-76 (2000).
5. K. Ogata, K. Sakurai, Sz.Fujita, Sg. Fujita, and K. Matsushige, *J. Cryst. Growth* **214 – 215** 312-315 (2000).

Downloaded 09 Aug 2010 to 120.140.165.57. Redistribution subject to AIP license or copyright; see http://proceedings.aip.org/proceedings/cpcr.jsp